PCCP

ROYAL SOCIETY OF CHEMISTRY

PAPER

View Article Online
View Journal | View Issue

Cite this: *Phys. Chem. Chem. Phys.*, 2024, **26**, 29003

Density scaling and isodynes in glycerol–water mixtures†

David B. Noirat,[ab] Bernhard Frick,[b] Bo Jakobsen,[a] Markus Appel[b] and Kristine Niss*[a]

Received 30th May 2024,
Accepted 4th November 2024

DOI: 10.1039/d4cp02231a

rsc.li/pccp

This paper presents dielectric and neutron spectroscopy data on two different glycerol–water mixtures at elevated pressures. Glycerol–water liquid mixtures have a high concentration of hydrogen bonds which usually is expected to lead to complex dynamics. However, with regard to the pressure dependence of the dynamics we reveal a surprisingly simple picture. Different aspects of the dynamics have the same pressure dependence, in other words the phase diagram of the liquids have so-called isodynes, density scaling is also observed to hold reasonably well and there is even some reminiscence of isochronal superposition. This suggests that these aspect of liquid dynamics are very general and hold for different types of intermolecular interactions.

I. Introduction

Both the properties of liquids and the transition from the liquid state into the non-equilibrium amorphous solid – the glass – are governed by the liquid dynamics. It is therefore important to understand liquid dynamics both from an application and a fundamental point of view. Some key features of liquid dynamics are universal: all liquids have a relaxation seen in the fluctuation and in the linear response and the characteristic time scale of this relaxation increases with decreasing temperature as well as with increasing pressure. In the low-viscosity liquid the relaxation is merged with vibrations and happens on the picosecond time scale while in the deeply supercooled liquid the relaxation can be as slow as a kilosecond. When the liquid gets slower than this a glass is formed because the relaxation no longer happens on the time scale we can practically observe.[1–4] While the above scenario is completely general there are also a lot of dynamical features that are specific for each liquid. The exact form of the temperature and density dependence differs from liquid to liquid and the spectral shape of the relaxation differs. In fact the relaxation is often (but not always) multi-modal exhibiting relaxation that can be both faster and slower than the main relaxation. A point of focus in research on liquid dynamics is to determine which features of liquid dynamics are general and which are specific either to a class of liquids or to one specific system. In this context hydrogen bonding liquids and specifically water are believed to have specific features connected to the network formation and directional character of the hydrogen bonds. The motivation for this study on glycerol–water mixtures is to add to the knowledge on how the hydrogen bonding network affects the pressure dependence of the dynamics.

Glycerol (propane-1,2,3-triol) is a molecular liquid with very good glass-forming ability and is readily studied by many experimental techniques, for example it yields a prominent signal in dielectric spectroscopy. It is probably for these reasons that it has become one of the most used liquids in fundamental studies of glassy dynamics.[5–10] Glycerol also has important applications, particularly in use as a cryoprotectant,[11–13] which means that understanding glycerol and glycerol in interaction with water is not only of fundamental scientific interest. There is a three dimensional hydrogen-bonding network in glycerol[14] and it is *via* hydrogen bonds that glycerol has its dominant interaction with water.[15–18] Glycerol has earlier been considered to be an archetypical glass-forming liquid, however today it is regarded as an example of a liquid with complicated dynamics, where the influence of the hydrogen bonding network plays an important role.[19,20]

Both the structure and dynamics of glycerol–water mixtures have been studied with a number of techniques.[16–26] It is well established that there is an eutectic point at a 0.28 molar fraction of glycerol. At lower glycerol concentrations the mixture is no longer a good glass-former and the liquid tends to phase separate and crystallize. It has also been claimed to have a liquid–liquid phase transition in this water rich regime.[25] In this work we focus on mixtures in the glycerol rich part of the phase diagram where the liquid is easy to supercool all the way

[a] "Glass and Time", IMFUFA, Department of Science and Environment, Roskilde University, Postbox 260, DK-4000 Roskilde, Denmark. E-mail: kniss@ruc.dk
[b] Institut Laue-Langevin, 71 avenue des Martyrs, CS 20156, 38042 Grenoble Cedex 9, France

† Electronic supplementary information (ESI) available. See DOI: https://doi.org/10.1039/d4cp02231a

into the glass. Previous studies of the shear mechanical response in glycerol rich water mixtures have shown that there is a dynamic transition around 0.5 molar fraction of glycerol.[19] In neat glycerol as well as in the mixture with glycerol concentration above 0.5 molar fraction the shear mechanical data reveal a dynamical mode slower than the alpha relaxation. This mode is believed to be due to the dynamics of the hydrogen bonding network and disappears quite abruptly with higher water concentration. The slow mode is not seen directly in the dielectric signal, though it has been suggested based on comparing light scattering and dielectric data that the main peak in the dielectric signal is in fact a slow mode from the hydrogen bond dynamics merged with the main alpha peak.[20] In the dielectric data there is a mode faster than the main relaxation appearing as water concentration increases.[19,25] This mode appears around the same point where the slow mode disappears in the shear mechanical signal, *i.e.* around 0.5 molar ratio. In this work we will extend the studies of glycerol–water mixtures with high pressure dielectric spectroscopy and quasielastic neutron scattering. Due to the qualitative change in behavior at 0.5 molar fraction glycerol we have chosen a concentration below and one above this threshold (0.4 molar fraction glycerol and 0.7 molar fraction glycerol).

Over the past two decades it has been established that the dynamics of liquids measured at high pressures is simplest to understand by viewing it as a function of temperature and density (rather than pressure).[27–29] For a large class of liquids it is found that the relaxation time and viscosity depend on a single scaling variable $\Gamma = \rho^{\gamma}/T$ where ρ is density, T is temperature and γ is a material specific constant.[28,30,31] This result is referred to as density scaling or thermodynamic scaling. In addition it is also found that the spectral shape of the relaxation is invariant along lines in the thermodynamic phase diagram where the relaxation time is constant.[32–34] This is referred to as isochronal superposition. Since the relaxation time only depends on Γ in many liquids isochronal superposition also means that the shape parameters describing the relaxation function depend only on Γ.

In the first papers that were based on quasielastic neutron scattering on *ortho*-terphenyl,[35,36] a van der Waals bonded glass-forming liquid, density scaling and isochronal superposition were interpreted in terms of a soft sphere intermolecular potential. In a soft sphere model liquid these results can be shown analytically and are exact. Later they have been explained in terms of isomorph theory, which is a more general framework in which the soft sphere model is contained as a special case.[37,38] The main prediction of isomorph theory is the existence of isomorphs. Isomorphs are lines in the phase diagram along which all structural and dynamical quantities are invariant, and isochronal superposition and density scaling follow as a consequence. Neither the soft sphere picture nor isomorph theory is expected to work in liquids where the intermolecular interactions are strongly directional as it is the case in hydrogen-bonding liquids.

Density scaling and isochronal superposition has been shown to break down to some extent in hydrogen-bonding systems[39,40] for example in glycerol at very high pressures.[41] However, these simple results appear to work surprisingly well also in hydrogen-bonding[33,42] liquids particularly far from the glass transition in the non-viscous liquid.[34] The largest difference between hydrogen-bonding liquids and van der Waals bonded liquids seems to be that the density scaling exponent, γ, has a much lower value in the hydrogen-bonding liquids where it is often close to 1, while it is usually above 4 in van der Waals bonded liquids.[28]

A result which is related to isochronal superposition is the finding that different relaxation processes and transport properties are constant along the same lines in the phase diagram – they have the same iso-lines. Sometimes this is shown by demonstrating that different properties obey density scaling with the same scaling exponent γ[32,43,44] or it is shown by tracking out the different isochrones in the phase diagram and showing that they collapse.[45,46] Recently, it has been suggested to refer to "isodynes" when several (or all) dynamical properties and transport coefficients of a system are constant along the same lines in the phase diagram.[46] If a system has isomorphs then these isomorphs are also isodynes – but as for density scaling and isochronal superposition, isodynes appear to exist also in systems that are not expected to obey to isomorph theory. Particularly in the example of an ionic liquid in ref. 46 it has been demonstrated that the structure changes along the isodynes which clearly shows that the isodynes are not isomorphs.

Water models have been used in simulations as the archetypal example of a liquid that does not obey isomorph theory,[37] thus if density scaling and isochronal superposition work for water it suggests that there is either a different or a more general explanation. Due to the crystallization it is not feasible to study density scaling of water close to the glass transition, but glycerol–water mixtures represent a highly complex system with large hydrogen-bonding concentration in which isomorph theory is not expected to work. Thus, the purpose of this work is to study the degree of density scaling, isochronal superposition and the existence of isodynes in glycerol–water mixtures.

II. Experiments

The two samples studied in these experiments are different mixtures of water and glycerol. The first has a glycerol molar ratio of 40% (x_{gly} = 0.4), and the second a glycerol molar ratio of 70% (x_{gly} = 0.7). Glycerol was sourced from Sigma (purity $\geq$99.5, water $\leq$0.1%), water is taken from a Milli-Q system. Mixtures were prepared in batches of *ca.* 10 mL in a glove bag. The amount of sample in the cell is *ca.* 1.5 mL.

The sample cell used for both neutron scattering and dielectric spectroscopy is a specific simultaneous dielectric and neutron scattering high pressure cell for pressures up to 4 kbar.[47] It contains the sample in an annular geometry with 12 mm diameter and a total thickness of 0.3 mm, of which a layer of 0.15 mm is used as cylindrical capacitor for the dielectric measurement. The temperature was controlled using a standard orange cryostat.

Dielectric spectroscopy data was recorded using a Novocontrol Alpha-A analyzer and a ZG4 extension. The total length of

cable from the analyzer to the capacitor in the cryostat is about 2.5 m.

Neutron scattering and dielectric data shown in Section III C are obtained on the cold neutron backscattering spectrometer IN16B at the Institute Laue-Langevin (Grenoble, France), using its standard setup with Si 111 crystal analysers and Doppler monochromator during several measurement campaigns.[48–50] The instrumental energy resolution was about 0.7 μeV and the accessible Q-range 0.2 $Å^{-1}$ to 1.8 $Å^{-1}$. Combined elastic and inelastic fixed window scans[51] enable to efficiently record the scattered neutron intensity at 0 μeV and 3 μeV energy transfer at counting times of 30 s and 2 min per point, respectively, while continuously cooling the sample along different isobars at a rate of 0.4 K min^{-1}. The measurement protocol applied in this case was to increase pressure at room temperature and then record data in cooling at constant pressure. Subsequently, full energy transfer spectra within ±30 μeV are recorded for 4 h at selected state points (T, p).

The dielectric data recorded simultaneously during neutron experiments serves mainly as additional observable of the sample state, *e.g.* to detect unwanted crystallization or identify technical problems with the pressure cell. More extensive data using dielectric spectroscopy as shown in Sections III A and III B are recorded separately with 90 minutes stabilisation times ensuring thermal equilibrium of the pressure cell and the sample.

Density was measured in Roskilde in a range 0.1–400 MPa and 245–315 K using a Unipress pressure vessel and a linear variable displacement transformer, see ref. 52. The values were extrapolated to lower temperature and to different pressures using the Tait equation with temperature given in K and pressure in MPa:

$$\rho = \frac{\rho_0}{\exp(\alpha(T - T_0)) \times \left(1 - A \times \ln\left(1 + \left(\frac{p}{b0 - b1 \times T}\right)\right)\right)}. \quad (1)$$

The Tait-equation parameters are shown in Table 1.

III. Results

A. Dielectric relaxation time – density scaling

Dielectric spectroscopy was performed along 7 isobars from ambient pressure to 300 MPa on the two glycerol–water mixtures x_{gly} = 0.4 and x_{gly} = 0.7. Fig. 1(a) and (b) show examples of the imaginary part of the dielectric constant as a function of frequency for different temperatures of an intermediate isobar. Each of the dielectric spectra exhibit a peak which is associated with the main relaxation in the liquid. The power law seen at low frequencies for the spectra taken at high temperatures is due to DC conductivity in the sample.

Fig. 1(c) and (d) show the frequency of the main peak, f_{max}, as a function of temperature for each of the isobars. It is seen that water has a plasticizing effect which corresponds to the glass transition decreasing by approximately 15 K when going from x_{gly} = 0.7 to x_{gly} = 0.4 consistent with ambient pressure results.[25]

The dynamics of both samples slow down as expected upon increased pressure. The effect of pressure is relatively moderate as it is often seen in hydrogen bonded liquids. By interpolating the data it is possible to estimate the position of isochrones, that is lines in the pressure–temperature phase diagram with the same relaxation time (or equivalently peak frequency) of the main relaxation. The glass transition line is an example of an isochrone, typically defined by the relaxation time being 1000 s. We find that the slope of the slow isochrones close to the glass transition is 0.04 K MPa^{-1} in both samples which is the same order as reported for pure glycerol (0.047 K MPa^{-1} in ref. 53) while it is a factor 2–3 lower than the typical isochrone slope in van der Waals bonded liquids.

In Fig. 2 we show the relaxation time defined as $\tau = 1/(2\pi f_{max})$, where f_{max} is the position of the maximum of the main relaxation seen in the imaginary part of the dielectric spectrum. Fig. 2(a) shows the so-called Angell plot where inverse temperature along each isobar is scaled with the pressure dependent glass transition temperature. We have pragmatically defined the glass transition at τ = 10 s to avoid extrapolation (rather than using the standard value τ = 1000 s). Glass forming liquids are traditionally characterized by the Fragility index which measures the slope in the Angell plot as the glass transition is approached from higher temperatures. It is seen in Fig. 2 that all the data collapse, which means that fragility is the same in the two samples and that it does not change significantly as a function of pressure. The fragility is 42 at 0.1 MPa and 47 at 400 MPa for a T_g of 10 s. For neat glycerol, literature gives a fragility of 52 at 0.1 MPa and 68 at 1.8 GPa for a T_g of 100 s.[41] Fig. 2(b) shows the relaxation times as a function of the density scaling parameter $\Gamma = \rho^{\gamma}/T$. The exponent γ is adjusted to get the best overlap of the data from different isobars. We find γ = 1.4 for x_{gly} = 0.7 and γ = 1 for x_{gly} = 0.4. The γ-value is determined by manually adjusting until the best overlap is found. The precision from this procedure is ±0.1. With these γ-values the overlap of the data is good which indicates that these mixtures obey density scaling. It should be noted that the pressure range is limited, and the density range even more so, with a density difference between the highest and lowest density of 6.4% for x_{gly} = 0.4 and 6% for x_{gly} = 0.7. It is possible that this power law density scaling breaks down at higher pressures, yet it is nevertheless a striking and practical representation of the data. The density scaling representation gives a direct measure of how big a role density plays compared to temperature in controlling the relaxation time, with a small value of γ indicating that the density is not very important. It is characteristic for hydrogen-bonding liquids that the scaling exponent values are around 1 while the value in van der Waals bonded liquids is generally above 4 and sometimes as high as 8. The reported scaling exponent of pure glycerol is γ = 1.4 (ref. 53),

Table 1 Tait equation parameters for the two water glycerol mixtures studied in this work. T_0 = 315 K

x_{gly}	α	A	$b0$	$b1$
0.4	4.1×10^{-4}	0.1349	786	0.0748
0.7	3.89×10^{-4}	0.0782	763	1.319

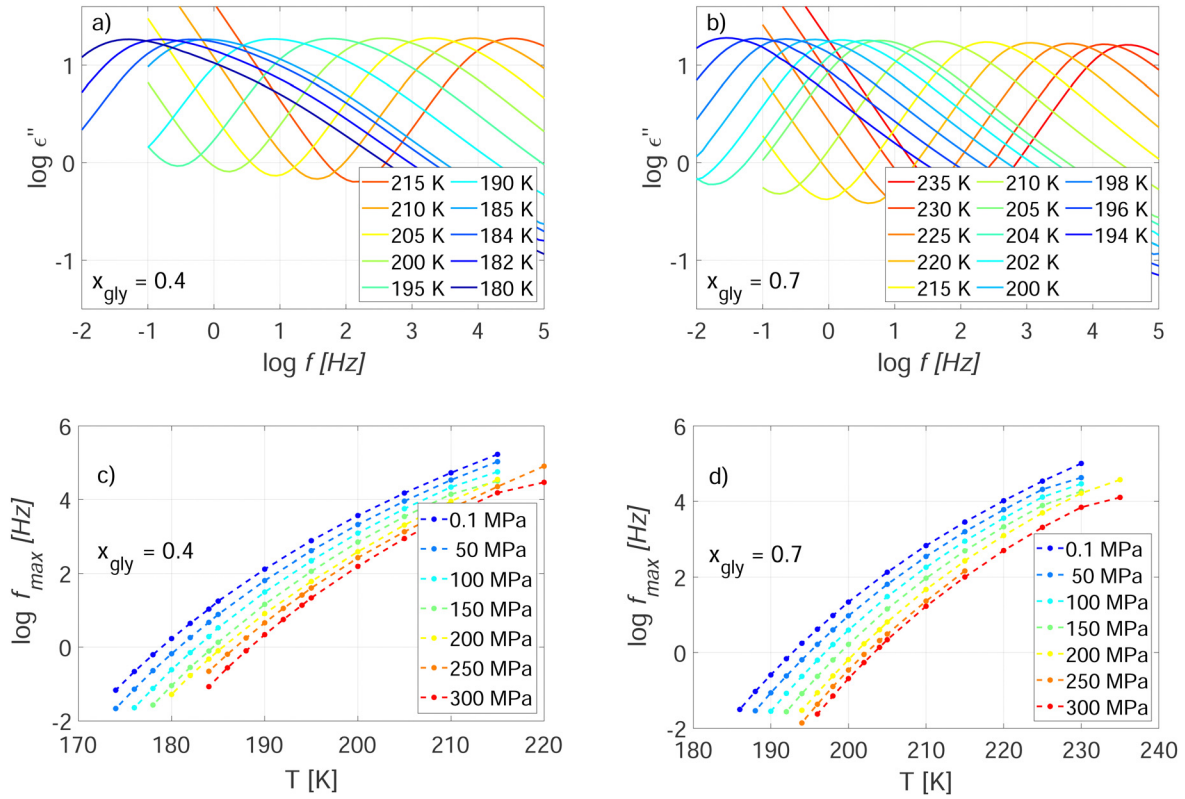

Fig. 1 Dielectric data of glycerol water mixtures with x_{gly} = 0.4 and x_{gly} = 0.7. (a) Imaginary part of the dielectric constant at 200 MPa and temperature in the range 180–215 K of the x_{gly} = 0.4 mixture. (b) Imaginary part of the dielectric constant at 200 MPa and temperature in the range 195–235 K of the x_{gly} = 0.7 mixture. (c) Position of the main peak in the imaginary part of the dielectric spectra, f_{max}, as a function of temperature along the isobars for the x_{gly} = 0.4 sample. (d) Position of the main peak, f_{max}, as a function of temperature along the isobars for the x_{gly} = 0.7 sample.

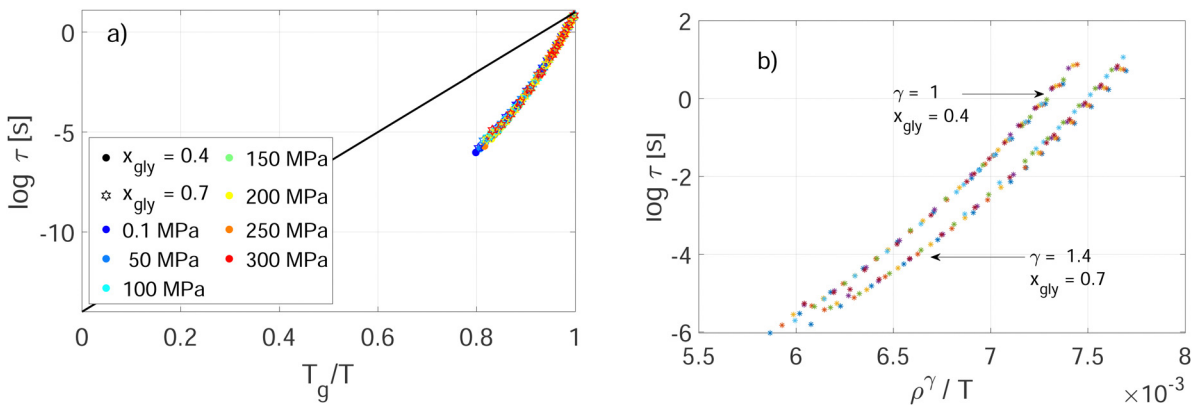

Fig. 2 The dielectric relaxation time defined as $\tau = 1/(2\pi f_{max})$ of glycerol water mixtures with x_{gly} = 0.4 and x_{gly} = 0.7. (a) Angell plot where temperature along each isobar is scaled with the pressure dependent glass transition temperature. We have pragmatically defined the glass transition at τ = 10 s to minimize extrapolation. (b) The relaxation times as a function of the density scaling parameter $\Gamma = \rho^{\gamma}/T$, where ρ is density, T, is temperature and γ is a free parameter. The parameter γ is adjusted to get the best visual overlap of the data from different isobars. We find γ = 1.4 for x_{gly} = 0.7 and γ = 1 for x_{gly} = 0.4.

and this could indicate that the exponent decreases as the water concentration, and hereby the hydrogen bonding concentration, increases.

B. Dielectric spectral shape – isochronal superposition

It is seen directly from the raw data in Fig. 1 that the dielectric spectra are broader in the sample with higher water content which is also well known from literature.[19,25] It is also clear, especially in the x_{gly} = 0.4 sample that the spectral shape broadens as the relaxation slows down upon cooling. The next question is what happens to the spectral shape when increasing pressure along an isochrone by keeping the relaxation time constant by simultaneously increasing temperature. To address this we have identified near-isochrone state points in our data

and plot the spectra of these in Fig. 3. The frequency axis is scaled with the peak position because the points are not exact isochrones (but isochrone within ±0.2 decades). It is immediately seen that the spectra do not collapse, which means that these mixtures do not obey isochronal superposition. Instead the spectra broaden on the high frequency flank as pressure is increased. This appears most pronounced in the x_{gly} = 0.4 sample and mainly at long relaxation times (low values of f_{max}), where the broadening evolves into a high frequency shoulder at high pressures (Fig. 3a). The evolution of a shoulder indicates that the broadening could be due to a process which can be considered to be separate from the main relaxation. Since the shoulder appears more pronounced in the sample with highest water content it is obvious to speculate that it could be the water dynamics separating from the glycerol dynamics. Another interpretation is that it may be a so-called Johari–Goldstein beta relaxation, which is an intrinsic faster relaxation found in many super-cooled liquids.[4]

We do not believe it is meaningful to fit these highly merged spectra, as it would require at least 6 parameters to capture two processes while the curves are rather featureless. To quantify the deviation from isochronal superposition we therefore move on in a model free direction by determining the width, $W_{1/2}$ of the spectra as defined in ref. 54. That is in terms of the logarithm of the half-width at half-maximum normalized to the half-width at half-maximum of a Debye relaxation and only including the high frequency side of the spectra because this is where the broadening is seen and to avoid any influence from DC conductivity.

Fig. 4(a) and (b) shows the $W_{1/2}$ value of the two mixtures along all the studied isobars as a function of temperature and relaxation peak frequency respectively. If there was isochronal superposition then the $W_{1/2}$ data should collapse when plotted as a function of peak frequency. While there is clear deviation from isochronal superposition it is also clear that the breadth measured in terms of $W_{1/2}$ changes less on an isochrone than it does on an isobar or an isotherm. Specifically for the x_{gly} = 0.4 sample, the $W_{1/2}$ value is seen to change by approx 2 along the isobars and up to 1.5 on the isotherms while the change is well below 1 on the isochrones and gets as low as 0.5 for the isochrones with short relaxation times/high f_{max}-values. In addition it appears that the x_{gly} = 0.7 sample is closer to having isochronal superposition than the x_{gly} = 0.4.

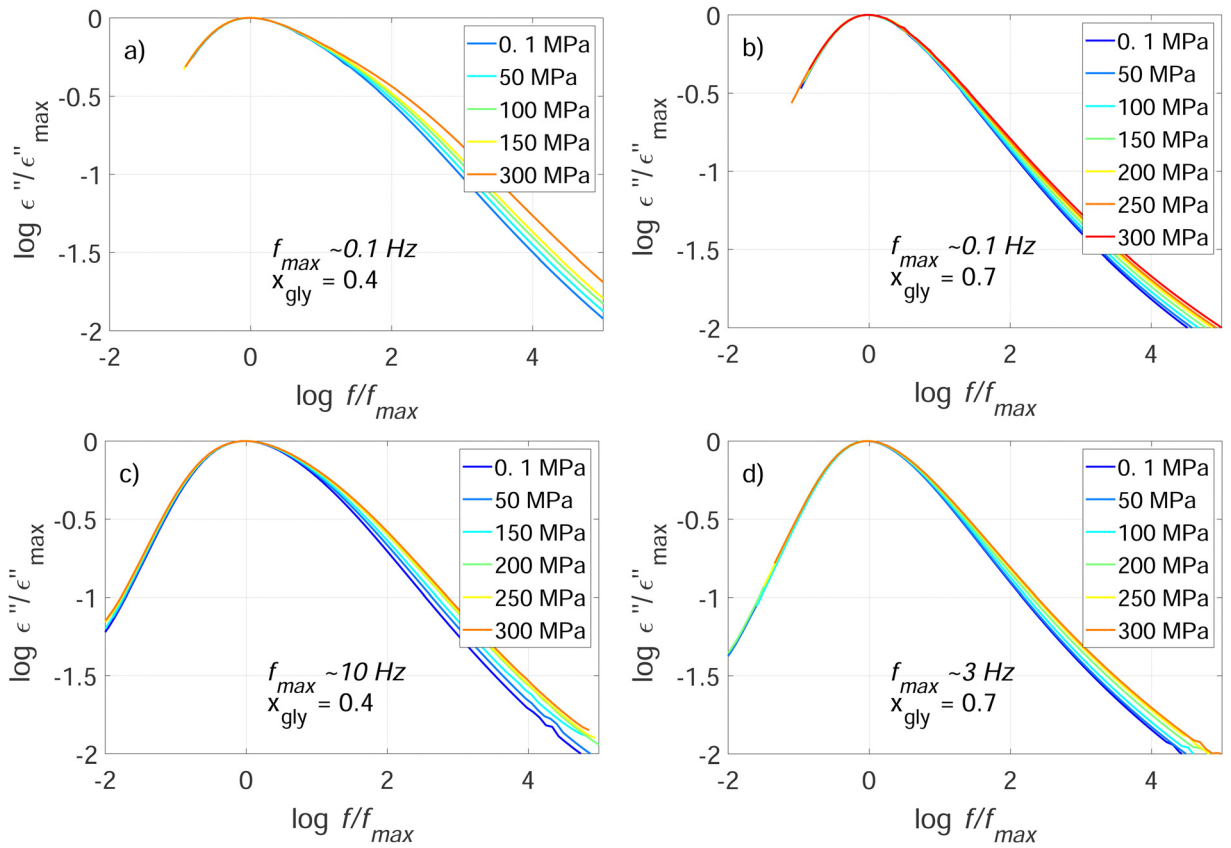

Fig. 3 Scaled dielectric spectra along isochrones (defined by $f_{max} = 1/(2\pi\tau)$ = constant within ±0.2 decades) of x_{gly} = 0.4 and x_{gly} = 0.7. (a) Imaginary part of the dielectric constant of x_{gly} = 0.4 at state points where $f_{max} \approx$ 0.1 Hz at pressures from 0.1 MPa to 300 MPa. (b) Imaginary part of the dielectric constant of x_{gly} = 0.7 at state points where $f_{max} \approx$ 0.1 Hz at pressures from P = 0.1 MPa to 300 MPa. (c) Imaginary part of the dielectric constant of x_{gly} = 0.4 at state points where $f_{max} \approx$ 10 Hz at pressures from P = 0.1 Mpa to 250 MPa. (d) Imaginary part of the dielectric constant of x_{gly} = 0.7 at state points where $f_{max} \approx$ 3 Hz at pressures from p = 0.1 MPa to 300 MPa.

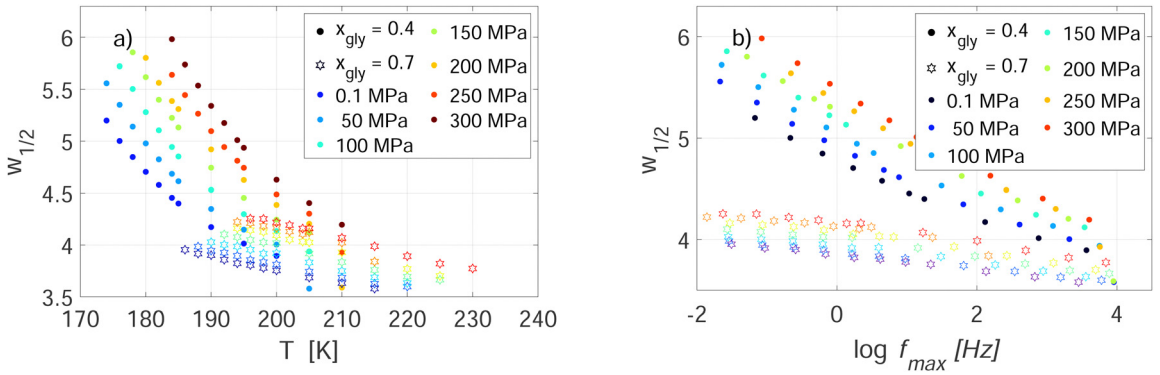

Fig. 4 (a) The $W_{1/2}$ value of x_{gly} = 0.4 and x_{gly} = 0.7 as a function of temperature. (b) The $W_{1/2}$ value of x_{gly} = 0.4 and x_{gly} = 0.7 as a function of frequency of the maximum in the imaginary part, f_{max}.

C. Combining dielectric and neutron spectroscopy

The main relaxation of the liquid moves out of the window of dielectric spectroscopy (which in our case stops at 1 MHz) at high temperatures where the liquid is non-viscous. In this range we can see the alpha relaxation by quasi elastic neutron scattering, which in the case of the backscattering instrument IN16B accesses the dynamics on the nano second time scale.

Fig. 5 shows elastic and inelastic fixed window scans[51] summed over all wave vectors, Q, of both samples at ambient pressure and at 400 MPa. Fig. 5(a) and (b) show the data as a function of temperature. The elastic intensity decreases as temperature increases due to the increased mobility of the molecules. The inelastic intensity, which is measured at an energy transfer of 3 μeV, has a peak at the temperature, where the relaxation is at a time scale of approximately 0.2 ns.

The data in Fig. 5 show that the dynamics on the nanosecond time scale is shifted to lower temperature when water content increases, which means that water has the expected plasticizing effect. Applying pressure slows down the dynamics, which is seen by a shift to higher temperature. This is of course

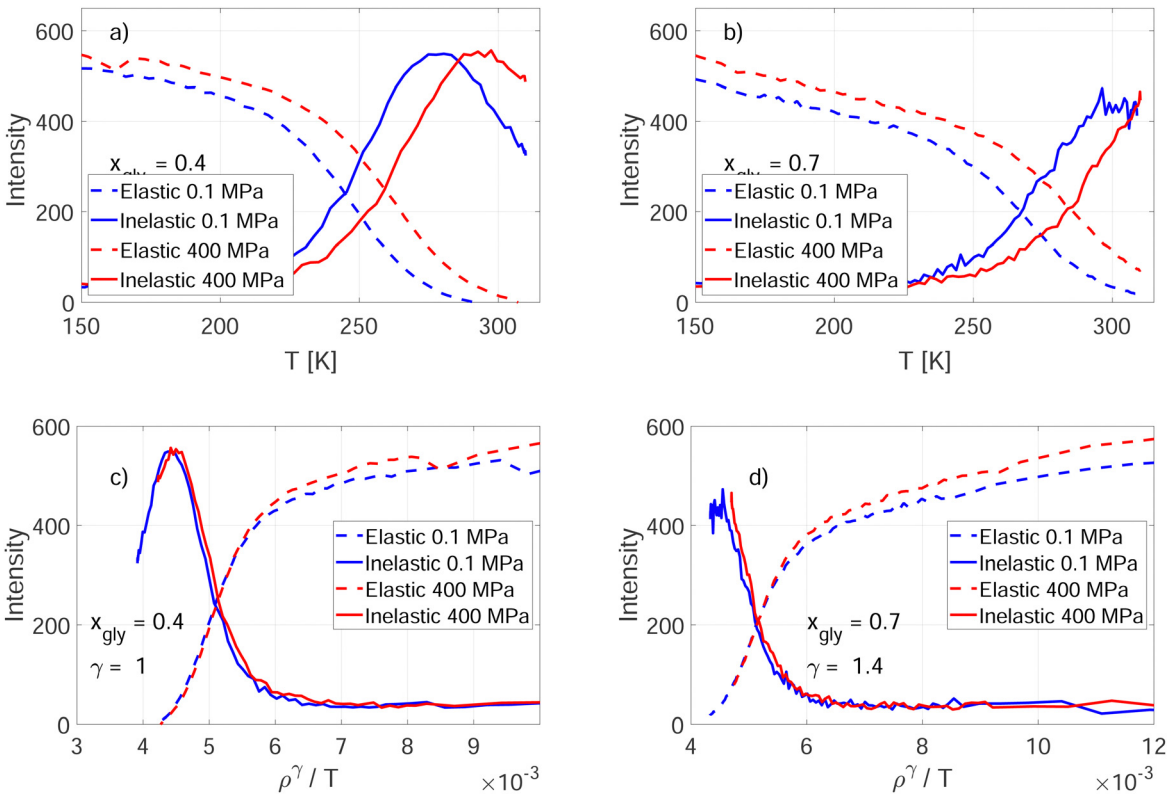

Fig. 5 Elastic and inelastic fixed window scans measured in IN16B in cooling summed over all wave vectors, Q. (a) Data from x_{gly} = 0.4 as a function of temperature. (b) Data from x_{gly} = 0.7 as a function of temperature. (c) Data from x_{gly} = 0.4 as a function of the density scaling variable ρ^{γ}/T using the value γ = 1 found from dielectric data in Fig. 2b. (d) Data from x_{gly} = 0.7 as a function of the density scaling variable ρ^{γ}/T using the value γ = 1.4 found from dielectric data in Fig. 2b.

also expected and it was also seen in the dielectric data in Section III A.

In ref. 34 it was found that the fixed window scan data obeyed density scaling with the same exponent as that dielectric data both for the van der Waals bonded liquid cumene and for the hydrogen bonding liquid dipropylene glycol. In Fig. 5(c) and (d) this approach is tested for the glycerol water samples, again using the scaling exponents found from density scaling of the dielectric data. It is found that this works quite well in collapsing the relaxation data for both samples. This indicates that the density scaling description of the super cooled dynamics can be extended to the fast dynamics at high temperatures.

The relaxation is, as mentioned, not in the window of the dielectric spectrometer at the temperatures and pressures where there is a quasielastic signal in the IN16B data. However, the dielectric data does show a clear conductivity signal. Conductivity is almost always seen in liquids, particularly hydrogen bonding liquids, at high temperatures and low frequencies. It is probably related to impurities which is indicated by the fact that it is not very reproducible when comparing two samples of the same liquid. In our data we also find that the conductivity is not reproducible in the sense that we get different results each time the cell is loaded. Yet, with one specific filling of the pressure cell the conductivity is reproducible when returning to a specific temperature–pressure point after cooling–heating and compression–decompression and we therefore only compare conductivity between measurements done on the exact same sample. Fig. 6 shows examples of the measured conductivity and illustrates how conductivity decreases when moving towards the more viscous liquid by increasing pressure or decreasing temperature. The figures also show examples of data from isoconductivity points – that is points in the temperature–pressure phase diagram where the conductivity is constant while temperature and pressure are different.

Fig. 7 shows quasielastic IN16B spectra taken simultaneously with the dielectric data in Fig. 6. It is immediately seen that the spectra taken on isoconductivity lines collapse. In the data of the x_{gly} = 0.4 sample the collapse is so good that the data from the two state points can not be distinguished from each other. In the case of the x_{gly} = 0.7 sample there is good overlap in the quasielastic signal while the elastic intensity is higher for the high pressure, high temperature, state point. However, in this case the conductivity is also slightly lower, indicating that we have not perfectly identified isoconductivity points. All in all we find that the isoconductivity points determined from data in the kHz range are also the isochrones in the nanosecond alpha relaxation seen in the incoherent neutron scattering signal. Conductivity is governed by the mobility of the ions which in turn is coupled to the viscosity of the liquid. For many electrolytes it is found that the molar conductivity and the inverse viscosity are either proportional or connected with a fractional exponent, referred to as the Walden Rule or a fractional Walden Rule. There are also examples where this has been found to hold as a function of pressure.[55,56] The result we find here may be related to the Walden Rule as the alpha relaxation, which we measure with neutron scattering, and the viscosity also are known to be closely coupled.[57] In this view it is expected that the conductivity and the alpha relaxation follow the same pressure dependence. It is however, worth noticing that we are comparing the microscopic alpha relaxation measured in a Q-range of 0.2 Å^{-1} to 1.8 Å^{-1} and a time scale of nanoseconds to the macroscopic conductivity measured at a time scale of milliseconds. Moreover, the neutron data do not only contain information of a time scale, but also a spectral shape. In other words, the collapse of the isoconductivity neutron scattering data in Fig. 7 can be seen as a generalization of isochronal superposition, since we find that both the relaxation time and the spectral shapes collapse for isoconductivity state points. This supports the finding in the dielectric data that the behavior moves towards a higher degree of isochronal superposition as the liquid becomes less viscous. From this we conjecture that these glycerol water mixtures have isodynes, in the low viscosity region of the phase diagram. 'Isodyne' is a term recently coined, as described in the introduction, to describe lines in the phase diagram along which several different dynamical properties are invariant.

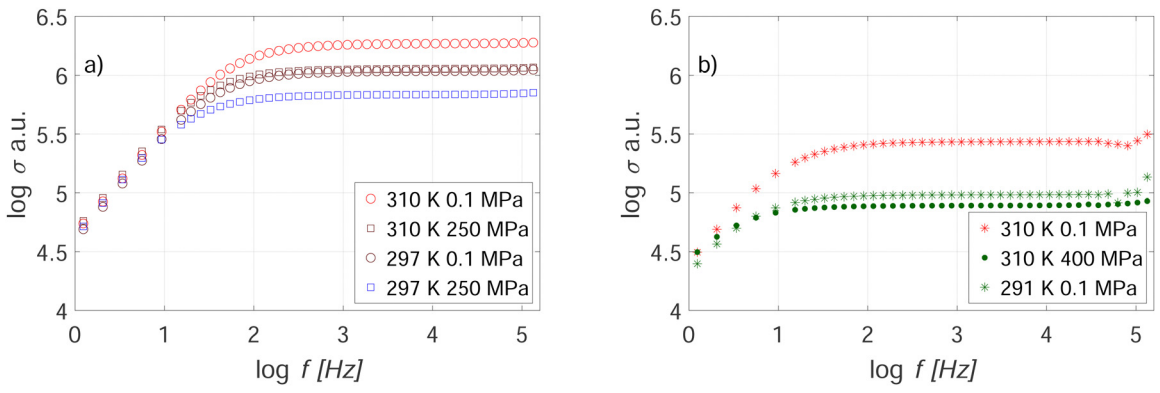

Fig. 6 High temperature dielectric data taken simultaneously with the neutron scattering data. The data is shown as the real part of the complex conductivity. The value at the plateau is the dc-conductivity. The bend down at low frequencies stems from electrode polarization. (a) x_{gly} = 0.4. Note that the two dark red sets of data from different pressure and temperature collapse indicating that these are isoconductivity state points. (b) x_{gly} = 0.7. The two green sets of data from different pressure and temperature (almost) collapse indicating that these are (near) isoconductivity state points.

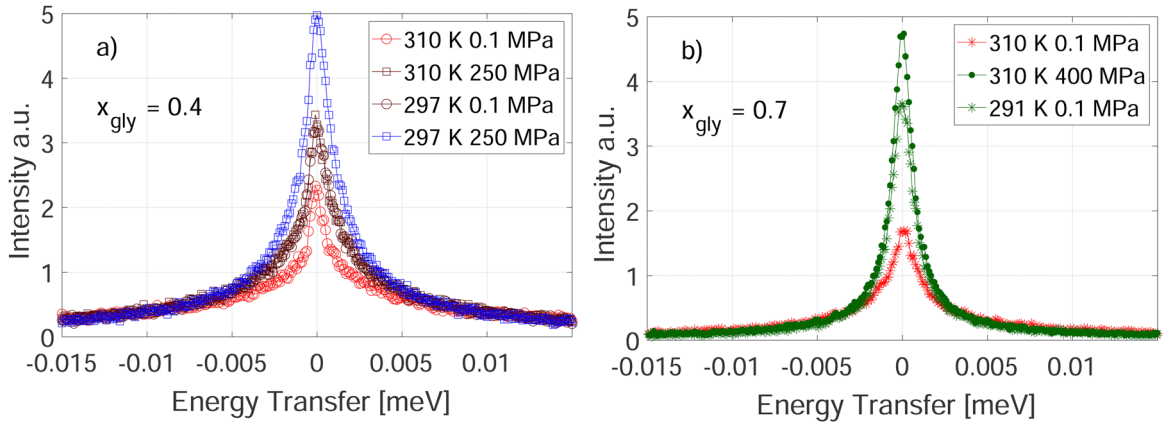

Fig. 7 Quasielastic neutron scattering data from IN16B taken simultaneously with the dielectric data in Fig. 6. (a) x_{gly} = 0.4. Note that there are two sets of dark red data taken at different pressures and temperatures with the same conductivity. These data collapse to a degree that makes it impossible to discern two curves. (b) x_{gly} = 0.7. There are two sets of green data taken at different pressures and temperatures with the same conductivity. These data collapse to a very high degree.

D. Analysis of neutron spectroscopy data

For further insight into the Q-dependent data from neutron spectroscopy experiments, we analyse the data in terms of a model function for the incoherent dynamic structure factor comprising the Fourier transform of a single stretched exponential process, also known as Kohlrausch–Williams–Watt (KWW) function:

$$S(Q,\omega,T) = A_1(Q)\mathcal{FT}\{\exp(-(t/\tau(Q,T))^{\beta})\} = A_1(Q)\mathrm{KWW}_{\tau(Q,T),\beta}(\omega) \quad (2)$$

where β is the stretching exponent, and $\tau(Q, T)$ the time constant of the process which depends both on scattering vector Q and temperature T. Given the fact that the temperature range where dynamics is probed in our neutron spectroscopy experiment ($T >$ 200 K) is well above the glass temperature of both samples, we approximate the temperature dependence of $\tau(Q, T)$ with a simple Arrhenius law:

$$\tau(Q, T) = \tau_0(Q)\exp(E_A/k_BT) \quad (3)$$

where E_A is the activation energy and $\tau_0(Q)$ a Q-dependent prefactor. We then fit the model from eqn (2) to multiple datasets at once in a global fit approach. Each dataset contains spectra for 15 different values of the scattering vector Q between 0.4 Å^{-1} and 1.85 Å^{-1} for fixed window scans at two energy offsets (3 μeV and 6 μeV) and full QENS spectra at 1–2 temperatures. Activation energy E_A and stretching parameter β are treated as global parameters with a unique value for the entire dataset, while prefactor $\tau_0(Q)$ and amplitude $A_1(Q)$ depend on the value of Q. Each spectrum is allowed to have an additional flat background, and the model function used for QENS spectra is further added a residual elastic contribution $A_0\delta(\omega)$ and convoluted with the experimentally measured resolution function of the instrument. Values of the KWW function are obtained using the numerical open-source implementation by Wuttke.[58]

We start by analysing each of our 4 datasets separately (x_{gly} = 0.4 and x_{gly} = 0.7, both at 0.1 MPa and 400 MPa), and find that β cannot reliably be obtained for higher pressures as the peak in the fixed window scan moves partially out of our accessible temperature range (see Fig. 5). Therefore, the value for β is obtained from the dataset at ambient pressure and fixed for the fit of the high pressure datasets. The fits of the above model describe the data exceptionally well (reduced χ^2 between 0.98 and 1.04), and while the resulting parameters for $\tau_0(Q)$ show a strongly dispersive behavior, they are very similar for both pressures (see Fig. 8). Guided by this observation, we decide to join the datasets for ambient and high pressure and ultimately fit all data for each sample simultaneously in a single fit by using only one set of parameters for $\tau_0(Q)$, but independent activation energies for ambient pressure and 400 MPa. An overview of the spectra for this final fit of both samples are shown in Fig. S1 and S2 (ESI†).

Our observation of pressure independent values of the prefactor $\tau_0(Q)$ in eqn (3) can also be related to the conjecture that density scaling works within the pressure–temperature region of

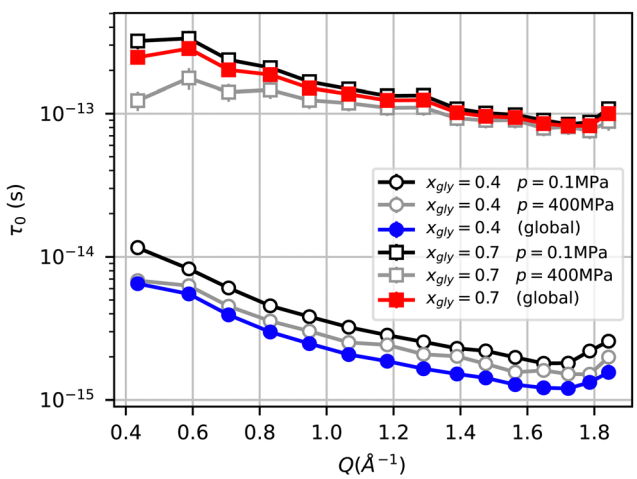

Fig. 8 Q-Dependence of prefactor τ_0 of the Arrhenius law governing the time constant of the KWW function as obtained from fit of neutron spectroscopy data. Results are shown for fits analyzing the datasets for different pressures individually (black and grey curves), and for global fit of both pressures simultaneously (red or blue curve).

Table 2 Resulting values of stretching exponent β and activation energy E_A from fits of neutron spectroscopy data for both glycerol–water samples. The last column shows the scaled density ratios between ambient and high pressure at 300 K (using γ = 1 for x_{gly} = 0.4 and γ = 1.4 for x_{gly} = 0.7)

x_{gly}	β	$E_A(0.1\ \text{MPa})/k_B$	$E_A(400\ \text{MPa})/k_B$	$\frac{E_A(400\ \text{MPa})}{E_A(0.1\ \text{MPa})}$	$\left(\frac{\rho(400\ \text{MPa})}{\rho(0.1\ \text{MPa})}\right)^{\gamma}$
0.4	0.59	5132(17) K	5432(17) K	1.059(5)	1.060
0.7	0.79	4399(22) K	4726(23) K	1.074(8)	1.085

our experiments. From the density curves $\rho(p, T)$ obtained for our samples using eqn (1) (see Fig. S3, ESI†), we can approximate the effect of pressure by a constant scaling factor between 200 K to 320 K, corresponding to the temperature range where dynamics is probed by our neutron spectroscopy experiments. Assuming that dynamics in our sample only depends on $\Gamma = \rho^{\gamma}/T$, a uniform scaling of the density ρ by the factor s would lead to an effective 'stretching' of the temperature scale by s^{γ}. This in turn means that in our fits using an Arrhenius law according to eqn (3), we can expect an increase in E_A by the factor s^{γ}, and no change in prefactor $\tau(Q)$ when pressure is applied. Table 2 shows the resulting parameters of our fit, as well as the ratios of activation energies between ambient pressure and 400 MPa, and values for s^{γ} obtained from the ratio of ρ at 300 K. Within the experimental errors in determining the activation energy, we find very good agreement of both ratios.

This agreement could in principle be expected given the collapse of the data in density scaling representation (*cf.* Fig. 5), but the fits described in this section show that the scaling also holds for the full set of Q-dependent data, *i.e.* resolved on length scales ranging from 4 Å to 15 Å.

IV. Discussion and conclusion

Studying the dielectric relaxation of glycerol water mixtures of concentration x_{gly} = 0.7 and x_{gly} = 0.4 in a pressure range up to 300 MPa we find that density scaling describes the behavior of the relaxation time well. We find scaling exponents to be γ = 1.4 for x_{gly} = 0.7 and γ = 1 for x_{gly} = 0.4. These scaling exponents are low as it is often found in hydrogen bonding systems. It does not seem meaningful to interpret these exponents as connected to the steepness of a repulsive potential as it has been done when connecting density scaling to soft sphere behavior or to isomorph theory.[37] This suggests that density scaling in hydrogen bonding liquids may either be due to a different mechanism or that there is a more general overlaying principle leading to density scaling. It is worth noticing that the data also collapse in the Angell plot (Fig. 2), and it may be possible that other phenomenological scalings could give a good collapse of the data. This suggests that the density scaling, found here in a limited density range, should not be overinterpreted.

Nevertheless density scaling represents a practical and interesting way of representing the data. It allows us to express the standard isobaric fragility, m_p, in these liquids in the following manner

$$m_p = m_\rho(1 + T_g\alpha_p\gamma) = m_\rho\left(1 + \left.\frac{d\log\rho}{d\log T}\right|_{T_g}\gamma\right) \quad (4)$$

where m_ρ is the isochoric fragility and α_p is the isobaric expansion coefficient.[59]

The effect of pressure on the relaxation time is relatively moderate for the glycerol water mixtures studied in this work and for hydrogen bonding liquids in general. This also means that isochoric and isobaric cooling leads to very similar behavior and thus that the two fragilities are close to each other. In terms of the expression in eqn (4) the explanation for this is that the effect of density on the relaxation time, which is quantified in the value of the density scaling exponent γ is small in these liquids.

The width of the dielectric spectra increases as a function of pressure along isochrones for both the studied glycerol–water mixtures but the effect is more pronounced in the x_{gly} = 0.4 sample than in the x_{gly} = 0.7 sample. Broadening in the spectra with increasing pressure along isochrones has also previously been reported for glycerol and 1,2,6-hexanetriol[39] and it is particularly pronounced in glycerol data obtained in the GPa-range.[41]

In the case of the x_{gly} = 0.4 sample, it is found that spectra collapse better at high temperatures and low pressures. In other words, isochronal superposition appears to work best in the low-viscosity liquid. As the liquid approaches the glass transition, the spectra broadens and this eventually develops into a high frequency shoulder, suggesting that the broadening is due to an additional process entering the signal. It is in these broad spectra that there is the strongest deviation from isochronal superposition. This could indicate that the main relaxation itself does obey a relatively high degree of isochronal superposition which would be in line with the findings in ref. 33 where isochronal superposition is found to hold for the main relaxation but not the beta relaxation in a hydrogen bonding system.

The dielectric spectra of hydrogen bonding liquids are in general narrow compared to the spectra of other liquids as well compared to the spectra of hydrogen bonding liquids themselves when measured with other techniques. An interpretation of this is that the narrow spectra are indeed a signature of the slow relaxation of the hydrogen bonding network similar to the Debye relaxation found in mono-alcohols.[20] In this interpretation, the narrowing of the spectra as the relaxation becomes faster is a signature that the alpha relaxation as well as possible beta relaxations get merged with and dominated by the Debye relaxation of the hydrogen bond network. Following this logic, the broadening of the spectra as pressure is applied could be due to the breaking up of the hydrogen bond network which means that the Debye signal from the relaxation of the hydrogen bond network becomes relatively weaker at high pressures.

In addition to a higher degree of isochronal superposition as the liquid relaxation gets faster, it is also seen in the low-viscosity liquid that isoconductivity lines collapse with isochrones of the dynamical structure factor. In other words, the non-viscous glycerol–water mixtures have isodynes. This again points to the dynamics getting simpler in the low-viscosity liquid where the main relaxation is dominating. The simple dynamics in the low-viscosity liquid is further substantiated by the fact that the neutron scattering data including both fixed

window scans and QENS spectra can be described by a global fit with a single Arrhenius KWW-function, with a sample specific stretching parameter and a pressure dependent activation energy.

In conclusion, we find that density scaling works for the two studied glycerol–water mixtures in the limited density range we access, but with low values of γ as it is often seen in hydrogen bonding liquids. While isochronal superposition does not hold in the glycerol–water mixtures there is some reminiscence of it, particularly in the non-viscous liquid, which indicates that isochronal superposition may hold for the main process. Moreover, we find that isoconductivity lines in the non-viscous liquids are also isochrones of the dynamical structure factor on the nanosecond timescale which suggests that the system has isodynes. Glycerol–water mixtures are liquids dominated by hydrogen bonds and their dynamics. The finding of simple features[4] such as the existence of isodynes, reasonably good density scaling as well as some degree of isochronal superposition is therefore quite surprising. The finding cannot be explained by isomorph theory and it suggests that this behavior in hydrogen bonding systems is either due to a different mechanism or that there is a more general underlying principle governing the density and temperature dependence of dynamics in liquids.

Data availability

The data for this article is available from the Glass and Time data repository **https://glass.ruc.dk/data**.

Conflicts of interest

There are no conflicts to declare.

Acknowledgements

We would like to thank the workshop at IMFUFA, RUC and the SANE group at the ILL for technical support.

References

1 J. C. Dyre, The glass transition and elastic models of glass-forming liquids, *Rev. Mod. Phys.*, 2006, **78**, 953–972.
2 L. Berthier and G. Biroli, Theoretical perspective on the glass transition and amorphous materials, *Rev. Mod. Phys.*, 2011, **83**, 587–645.
3 M. D. Ediger and P. Harrowell, Perspective: supercooled liquids and glasses, *J. Chem. Phys.*, 2012, **137**(8), 080901.
4 K. Niss and T. Hecksher, Perspective: searching for simplicity rather than universality in glassforming liquids, *J. Chem. Phys.*, 2018, **149**(23), 230901.
5 G. E. Gibson and W. F. Giauque, The third law of thermodynamics: evidence from the specific heats of glycerol that the entropy of a glass exceeds that of a crystal at the absolute zero, *J. Am. Chem. Soc.*, 1923, **45**, 93–104.
6 C. H. Wang and R. B. Wright, Raman Scattering Studies of Liquids and Glasses. I. Liquid and Super-cooled Liquid Glycerol, *J. Chem. Phys.*, 1971, **55**(4), 1617–1624.
7 B. Schiener, R. Bohmer, A. Loidl and R. Chamberlin, Nonresonant spectral hole burning in the slow dielectric response of supercooled liquids, *Science*, 1996, **11**(274), 752–754.
8 P. Lunkenheimer, U. Schneider, R. Brand and A. Loid, Glassy dynamics, *Contemp. Phys.*, 2000, **41**, 15–36.
9 T. Pezeril, C. Klieber, S. Andrieu and K. A. Nelson, Optical Generation of Gigahertz-Frequency Shear Acoustic Waves in Liquid Glycerol, *Phys. Rev. Lett.*, 2009, **102**, 107402.
10 S. Albert, T. Bauer, M. Michl, G. Biroli, J. P. Bouchaud and A. Loidl, *et al.*, Fifth-order susceptibility unveils growth of thermodynamic amorphous order in glass-formers, *Science*, 2016, **352**, 1308–1311.
11 R. W. Salt, Role of Glycerol in producing Abnormally Low Supercooling and Freezing Points in an Insect, Bracon cephi (Gahan), *Nature*, 1958, **181**, 1281.
12 J. L. Dashnau, N. V. Nucci, K. A. Sharp and J. M. Vanderkooi, Hydrogen Bonding and the Cryoprotective Properties of Glycerol/Water Mixtures, *J. Phys. Chem. B*, 2006, **110**(27), 13670–13677.
13 D. X. Li, B. L. Liu, Y. Shu Liu and C. Lung Chen, Predict the glass transition temperature of glycerol–water binary cryoprotectant by molecular dynamic simulation, *Cryobiology*, 2008, **56**(2), 114–119.
14 J. J. Towey, A. K. Soper and L. Dougan, The structure of glycerol in the liquid state: a neutron diffraction study, *Phys. Chem. Chem. Phys.*, 2011, **13**, 9397–9406.
15 J. J. Towey, A. K. Soper and L. Dougan, Preference for Isolated Water Molecules in a Concentrated Glycerol–Water Mixture, *J. Phys. Chem. B*, 2011, **115**(24), 7799–7807.
16 J. J. Towey and L. Dougan, Structural Examination of the Impact of Glycerol on Water Structure, *J. Phys. Chem. B*, 2012, **116**(5), 1633–1641.
17 J. J. Towey, A. K. Soper and L. Dougan, Molecular Insight Into the Hydrogen Bonding and Micro-Segregation of a Cryoprotectant Molecule, *J. Phys. Chem. B*, 2012, **116**(47), 13898–13904.
18 J. J. Towey, A. K. Soper and L. Dougan, What happens to the structure of water in cryoprotectant solutions?, *Faraday Discuss.*, 2013, **167**, 159–176.
19 M. H. Jensen, C. Gainaru, C. Alba-Simionesco, T. Hecksher and K. Niss, Slow rheological mode in glycerol and glycerol–water mixtures, *Phys. Chem. Chem. Phys.*, 2018, **20**, 1716–1723.
20 J. P. Gabriel, P. Zourchang, F. Pabst, A. Helbling, P. Weigl and T. Bohmer, *et al.*, Intermolecular crosscorrelations in the dielectric response of glycerol, *Phys. Chem. Chem. Phys.*, 2020, **22**, 11644–11651.
21 L. B. Lane, *Ind. Eng. Chem.*, 1925, **17**, 924.
22 Y. Hayashi, A. Puzenko, I. Balin, Y. E. Ryabov and Y. Feldman, Relaxation Dynamics in Glycerol–Water Mixtures. 2. Mesoscopic Feature in Water Rich Mixtures, *J. Phys. Chem. B*, 2005, **109**(18), 9174–9177.
23 A. Puzenko, Y. Hayashi, Y. E. Ryabov, I. Balin, Y. Feldman and U. Kaatze, *et al.*, Relaxation Dynamics in Glycerol–Water

Mixtures: I. Glycerol-Rich Mixtures, *J. Phys. Chem. B*, 2005, **109**(12), 6031–6035. PMID: 16851659.

24 A. Puzenko, Y. Hayashi and Y. Feldman, Space and time scaling in glycerol–water mixtures, *J. Non-Cryst. Solids*, 2007, **353**(47–51), 4518–4522Dielectric Relaxation and Related PhenomenaProceedings of the 4th Conference of the International Dielectric Society and the 9th International Conference on Dielectric and Related Phenomena4th Conference of the International Dielectric Society and the 9th International Conference on Dielectric and Related Phenomena.

25 I. Popov, A. G. Gutina, A. P. Sokolov and Y. Feldman, The puzzling first-order phase transition in water–glycerol mixtures, *Phys. Chem. Chem. Phys.*, 2015, **17**(27), 1–9.

26 J. Bachler, V. Fuentes-Landete, D. A. Jahn, J. Wong, N. Giovambattista and T. Loerting, Glass polymorphism in glycero–water mixtures: II. Experimental studies, *Phys. Chem. Chem. Phys.*, 2016, **18**, 11058–11068.

27 C. Alba-Simionesco, D. Kivelson and G. Tarjus, Temperature, Density, and Pressure Dependence of Relaxation Times in Supercooled Liquids, *J. Chem. Phys.*, 2002, **116**, 5033–5038.

28 C. M. Roland, S. Hensel-Bielowka, M. Paluch and R. Casalini, Supercooled dynamics of glass-forming liquids and polymers under hydrostatic pressure, *Rep. Prog. Phys.*, 2005, **68**, 1405–1478.

29 T. B. Schrøder, U. R. Pedersen, N. P. Bailey, S. Toxvaerd and J. C. Dyre, Hidden scale invariance in molecular van der Waals liquids: a simulation study, *Phys. Rev. E: Stat., Nonlinear, Soft Matter Phys.*, 2009, **80**, 041502.

30 C. Alba-Simionesco, A. Cailliaux, A. Alegrıa and G. Tarjus, Scaling out the denisty dependence of the α relaxation in glass-forming polymers, *Europhys. Lett.*, 2004, **68**, 58–64.

31 R. Casalini and C. M. Roland, Thermodynamical scaling of the glass transition dynamics, *Phys. Rev. E: Stat., Nonlinear, Soft Matter Phys.*, 2004, **69**, 062501.

32 K. L. Ngai and M. Paluch, Corroborative evidences of TVγ-scaling of the α-relaxation originating from the primitive relaxation/JG β relaxation, *J. Non-Cryst. Solids*, 2017, **478**, 1–11.

33 K. Adrjanowicz, J. Pionteck and M. Paluch, Isochronal superposition and density scaling of the intermolecular dynamics in glass-forming liquids with varying hydrogen bonding propensity, *RSC Adv.*, 2016, **6**, 49370–49375.

34 H. W. Hansen, B. Frick, S. Capaccioli, A. Sanz and K. Niss, Isochronal superposition and density scaling of the α-relaxation from pico- to millisecond, *J. Chem. Phys.*, 2018, **149**(21), 214503.

35 A. Tolle, H. Zimmermann, F. Fujara, W. Petry, W. Schmidt and H. Schober, *et al.*, Vibrational states of glassy and crystalline orthoterphenyl, *Eur. Phys. J. B*, 2000, **16**(1), 73–80.

36 A. Tolle, Neutron scattering studies of the model glass former *ortho*-terphenyl, *Rep. Prog. Phys.*, 2001, **64**, 1473–1532.

37 N. P. Bailey, U. R. Pedersen, N. Gnan, T. B. Schrøder and J. C. Dyre, Pressure-energy correlations in liquids. I. Results from computer simulations, *J. Chem. Phys.*, 2008, **129**(18), 184507.

38 N. Gnan, T. B. Schrøder, U. R. Pedersen, N. P. Bailey and J. C. Dyre, Pressure-energy correlations in liquids. IV.''Isomorphs'' in liquid phase diagrams, *J. Chem. Phys.*, 2009, **131**(23), 234504.

39 L. A. Roed, D. Gundermann, J. C. Dyre and K. Niss, Communication: two measures of isochronal superposition, *J. Chem. Phys.*, 2013, **139**, 101101.

40 H. W. Hansen, A. Sanz, K. Adrjanowicz, B. Frick and K. Niss, Evidence of a one-dimensional thermodynamic phase diagram for simple glass-formers, *Nat. Commun.*, 2018, **9**, 518.

41 S. Pawlus, M. Paluch, J. Ziolo and C. M. Roland, On the pressure dependence of the fragility of glycerol, *J. Phys.: Condens. Matter*, 2009, **21**(33), 332101.

42 M. Romanini, M. Barrio, R. Macovez, M. D. Ruiz-Martin, S. Capaccioli and J. L. Tamarit, Thermodynamic Scaling of the Dynamics of a Strongly Hydrogen-Bonded Glass-Former, *Sci. Rep.*, 2017, **7**(1), 1346.

43 T. C. Ransom and W. F. Oliver, Glass Transition Temperature and Density Scaling in Cumene at Very High Pressure, *Phys. Rev. Lett.*, 2017, **119**, 025702.

44 H. W. Hansen, F. Lundin, K. Adrjanowicz, B. Frick, A. Matic and K. Niss, Density scaling of structure and dynamics of an ionic liquid, *Phys. Chem. Chem. Phys.*, 2020, **22**, 14169.

45 L. A. Roed, K. Niss and B. Jakobsen, Communication: high pressure specific heat spectroscopy reveals simple relaxation behavior of glass forming molecular liquid, *J. Chem. Phys.*, 2015, **143**(22), 221101.

46 P. A. Knudsen, K. Niss and N. P. Bailey, Quantifying dynamical and structural invariance in a simple molten salt model, *J. Chem. Phys.*, 2021, **155**(5), 054506.

47 A. Sanz, H. W. Hansen, B. Jakobsen, I. H. Pedersen, S. Capaccioli and K. Adrjanowicz, *et al.*, Highpressure cell for simultaneous dielectric and neutron spectroscopy, *Rev. Sci. Instrum.*, 2018, **89**(2), 023904.

48 H. W. Hansen, M. Appel, B. Jakobsen, K. Niss and D. Noirat, *Recovering of density scaling and isochronal superposition by globular dynamics of dipropylene glycol*, Institut Laue-Langevin (ILL), 2019, DOI: **10.5291/ILLDATA.6-05-998**.

49 K. Niss, C. A. Simionesco, M. Appel, B. Frick, H. W. Hansen and T. Hecksher, *et al.*, *How independent is water dynamics in liquid glycerol–water mixtures?*, Institut Laue-Langevin (ILL), 2020, DOI: **10.5291/ILL-DATA.6-05-1008**.

50 D. Noirat, M. Appel, B. Frick and K. Niss, *Dynamics of glycerol–water mixture at 0.7 molar ratio in the temperature and pressure dimension*, Institut Laue-Langevin (ILL), 2020, DOI: **10.5291/ILL-DATA.6-05-1012**.

51 B. Frick, J. Combet and L. van Eijck, New possibilities with inelastic fixed window scans and linear motor Doppler drives on high resolution neutron backscattering spectrometers, *Nucl. Instrum. Methods Phys. Res., Sect. A*, 2012, **669**, 7–13.

52 L. A. R. Schmidt, *Simplicity of supercooled liquids: Experimental investigations inspired by the isomorph theory*, [PhD thesis], Roskilde University, Denmark, 2018.

53 A. Reiser, G. Kasper, C. Gainaru and R. Bohmer, Communications: high-pressure dielectric scaling study of a monohydroxy alcohol, *J. Chem. Phys.*, 2010, **132**(18), 181101.

54 A. I. Nielsen, T. Christensen, B. Jakobsen, K. Niss, N. B. Olsen and R. Richert, *et al.*, Prevalence of approximate t

relaxation for the dielectric α process in viscous organic liquids, *J. Chem. Phys.*, 2009, **130**(15), 154508.

55 D. Reuter, P. Munzner, C. Gainaru, P. Lunkenheimer, A. Loidl and R. Bohmer, Translational and reorientational dynamics in deep eutectic solvents, *J. Chem. Phys.*, 2021, **154**(15), 154501.

56 M. Musial, S. Bair, S. Cheng, Z. Wojnarowska and M. Paluch, FractionalWalden rule for aprotic ionic liquids: experimental verification over a wide range of temperatures and pressures, *J. Mol. Liq.*, 2021, **331**, 115772.

57 B. Jakobsen, T. Hecksher, T. Christensen, N. B. Olsen, J. C. Dyre and K. Niss, Communication: identical temperature dependence of the time scales of several linear-response functions of two glassforming liquids, *J. Chem. Phys.*, 2012, **136**, 081102.

58 J. Wuttke, Laplace–Fourier Transform of the Stretched Exponential Function: Analytic Error Bounds, Double Exponential Transform, and Open-Source Implementation ''libkww'', *Algorithms*, 2012, **5**(4), 604–628.

59 K. Niss and C. Alba-Simionesco, Effects of density and temperature on correlations between fragility and glassy properties, *Phys. Rev. B: Condens. Matter Mater. Phys.*, 2006, **74**, 024205.

